An Improved SLIC Algorithm for Segmentation of Microscopic Cell Images

Fuyun He[1], M A Parvez Mahmud[2], Abbas Z. Kouzani[2], Adnan Anwar[2], Frank Jiang[2,*], Sai Ho Ling[3,*]

[1]College of Electronic Engineering, Guangxi Normal University, Guilin, China

[2]Faculty of Science, Engineering & Built Environment, Deakin University, Australia

[3]Faculty of Engineering and IT, University of Technology Sydney, Australia

*Corresponding authors: Steve.Ling@uts.edu.au ; Frank.Jiang@deakin.edu.au

Abstract: Accurate nuclear and cell segmentations plays an important role in improving the accuracy of target recognition in microscopic cell images. As the traditional SLIC (Simple Linear Iterative Clustering) algorithm cannot segment microscopic cell images well, an improved SLIC superpixel segmentation algorithm based on gray scale enhancement and regional equalization is proposed. According to the characteristics of microscopic cell images, selecting different transformation parameters with the conditional iterative algorithm, the best classification multi-threshold method based on maximum entropy criterion is used to nonlinearly enhance the gray scale of the original images, while enhancing the contrast of the image, it also greatly improves the balance of each classification region. Then the gray distance and spatial distance are calculated respectively in the circle neighborhood of the cluster center to realize the superpixel segmentation of the image. Finally, the improved SLIC algorithm and the comparison algorithm are tested and evaluated. The experimental results show that our improved SLIC algorithm model has higher segmentation accuracy and is more suitable for cell segmentation in microscopic cell images than original SLIC algorithm.

Keywords: Cell segmentation; Superpixel; SLIC algorithm; Pathological images

1. Introduction

With the rapid development of artificial intelligence, machine learning, computer vision and other theories and technologies, automatic recognition and analysis of histopathological images have been applied more and more widely, which has become a hot issue in academic and industry communities [1-3]. In medical pathological image analysis, the precise segmentation of cell and nucleus is one of the most basic and important fields and the starting point for a variety of computational pathology applications, which is the basic premise of identifying and analyzing pathological cell images, such as nuclear morphological analysis, cell type classification and cancer grading [4-6]. The main challenge of microscopic cell image segmentation lies in the random movement of cells from the influence of their physiological environment during the slicing, and the microscopic imaging mode, microscope magnification, cell type and other different factors [7]. These factors leaded to the existence of adhesion or overlap of cells, different shapes and sizes of cells, different light and shade, different color, different nuclear morphology and so on. In addition, the texture, folds, impurities and other phenomena in the cytoplasm around the cell will also affect the segmentation accuracy [8, 9]. Therefore, for the segmentation of microscopic cell images, our focus of this paper is how to solve the problems of sample images and improve the segmentation accuracy.

The early methods for cell image segmentation, which limited by computing power and sample counts, mainly adopted the traditional segmentation algorithm. According to the color, contour, texture and other characteristic information of the cell sample image, the image is divided into different regions. The same region contains the same semantic information, and there are certain differences between different regions [10], such as Gregoretti et al. proposed an automatic segmentation method to detect the regions isolated

from nuclear regions in high-resolution fluorescent cell image sequences. It is an integrated method, which used classification techniques and active contour models to better understand the 3D distribution of Subcellular in living cell image sequences [11]. These traditional methods are mainly based on threshold, edge detection and region growth and so on [12-14].The threshold segmentation algorithm is simple in implementation, small scale in computation and stable in performance, but it does not consider the spatial characteristics of images, so it is sensitive to noise, and it is very poor segmentation effect for images with dense cell distribution. The edge detection algorithm uses various convolution operators to identify the differences in edge pixels between different regions. In essence, the first order differential extreme point and the second order differential zero crossing in the differential method are used to determine the edges between different regions, and then the region to which the pixel belongs is determined according to the closed edge [15]. This algorithm has high time and space complexity, and each type of convolution operator is only effective for specific problems and not very ideal for more complex cell image segmentation effect. Watershed segmentation is the most widely used region growth algorithm with an excellent response to weak edges and can obtain closed continuous edges, however, it is necessary to predefine boundary initialization parameters and requires great computing power, and it is prone to over-segmentation for cell image segmentation [16].

Image superpixel segmentation refers to the segmentation of image into polygon image cluster composed of multiple adjacent pixels by using the information of brightness, color and space of image. Image superpixel segmentation plays an important role in the field of computer vision and is widely used in target recognition, target tracking and target classification [17-19]. Ren et al. first clarified the concept of superpixel, which refers to the image cluster assembled by adjacent pixels with similar brightness, color, texture and other features [20]. Superpixel segmentation can reduce the size of processing objects and reduce the information redundancy of subsequent image processing and analysis to improve the overall speed of image processing. The application value of superpixel in computer vision determines that the superpixel algorithm must have accurate clustering results and efficient processing speed. Superpixel segmentation algorithms are mainly classified into graph theory and gradient descent method. Graph theory method mainly includes graph-based method, Ncut method and Super Pixel Lattice method [21]. Gradient descent method mainly includes Mean Shift method [22], Turbo pixels method [23], and Simple Linear Iterative Clustering (SLIC) algorithm [24].SLIC can obtain the result of superpixel segmentation with regular shape and uniform size, and has a good effect of fitting the strong edge of image.However; SLIC is sensitive to the setting of the number of superpixels. If the number of superpixels is set too small or too large, it is easy to cause under-segmentation or over-segmentation of the image [25].

The SLIC algorithm is used for segmentation based on the similarity of LAB color and spatial distance. Its advantages of short time consumption, uniform size of superpixel block, and regular contour are widely used in color image, optical remote sensing, natural scene, and other image segmentation tasks. However, the number of superpixels in the superpixel segmentation method is sensitive, and it is difficult to fit the weak target boundary of microscopic cell image effectively, and it is easy to cause the problems of under-segmentation or over-segmentation [23, 24]. Therefore, we proposed to integrate the gray-scale enhancement with the superpixel clustering algorithm. Firstly, maximum entropy principle and gray scale transformation were used to enhance the contrast of microscopic cell images. On the basis of maximum entropy principle, the optimal classification of image gray level was carried out by conditional iteration algorithm; the corresponding gray transformation is carried out for each classification region. Then, on the basis of great improvement of image contrast enhancement and region equalization, we simplified the 5D SLIC to 3D SLIC and performed superpixel clustering segmentation on two microscopic cell image sets. Finally, the segmentation results of the improved method and the original method were compared and

analyzed.

The rest of this paper is organized as follows. In Section 2, the basic pipeline of SLIC superpixel segmentation algorithm is described. In Section 3, according to the characteristics of microscopic cell imaging, an improved model of SLIC algorithm is proposed. In Section 4, the experimental results and analysis are presented. Section 5 summarizes the conclusions of this paper and puts forward the future research work.

2. SLIC superpixel segmentation algorithm

A superpixel is a small area consisting of adjacent pixels with similar color, brightness, texture, and other characteristics. Most of these small regions retain the effective information for further image segmentation and generally do not destroy the boundary information of objects in the image. Superpixel is to divide a pixel-level map into a district-level map, which is an abstraction of basic information elements [26, 27].

According to the predetermined number of superpixels *M*, the SLIC firstly distributes seed points (cluster centers) evenly within the image. Assuming that the image has a total of *N* pixel points, and is pre-segmented into *M* superpixels of the same size, then the size of each superpixel is *N/M*, and the distance of adjacent seed points is $S=\sqrt{N/M}$ .Then, the feature vector of the cluster center is expressed as $C_i=[l_i,a_i,b_i,x_i,y_i]^T$, which is composed of the CIELAB space color value $[l_i,a_i,b_i]$ and the position (x_i,y_i) of the pixel. For getting better segmentation effect, the SLIC algorithm will also fine-tune each clustering center to the point with the lowest gradient in its 3×3 neighborhood according to the image gradient, so as to avoid inaccurate segmentation caused by clustering center falling on the edge. After the clustering center is initialized, the algorithm starts to cluster pixel points through iteration. Each pixel point is classified into the class with the nearest clustering center, and the distance between pixel points and the clustering center is calculated within $2S\times2S$ neighborhood of each clustering center, as shown in figure 1(a).

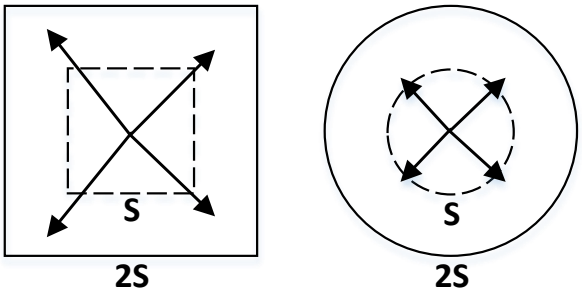

(a) (b)

Fig. 1 Comparison of search area between original SLIC and improved SLIC algorithm.
(a) Search area of original SLIC algorithm; (b) Search area of improved SLIC algorithm

In the SLIC algorithm, the distance between the candidate pixel and the cluster center is defined as,

$$d_s(i,j)=\sqrt{(x_i-x_j)^2+(y_i-y_j)^2} \tag{1}$$

$$d_c(i,j)=\sqrt{(a_i-a_j)^2+(b_i-b_j)^2+(l_i-l_j)^2} \tag{2}$$

$$d(i,j)=\sqrt{d_s^2+\alpha d_c^2} \tag{3}$$

where, i is the label of the clustering center, and j represents the one-dimensional index of all pixels in $2S\times2S$ neighborhood of the clustering center; $d_s(i,j)$ represents the spatial similarity between pixels;

$d_c(i,j)$ represents the color similarity between pixels; $d(i,j)$ represents the total similarity between the clustering center and pixel points, the smaller the $d(i,j)$, the more similar the pixel points are to the clustering center. $\alpha = s/m$, s is the size of the neighborhood of clustering center, and m is the compact factor, which is used to control the proportion of $d_s(i,j)$ and $d_c(i,j)$ in $d(i,j)$, and in general $s \in [1,40]$.

3. Improved SLIC algorithm based on microscopic cell images

When the traditional SLIC algorithm is applied to different segmentation objects, it generally needs to complete the whole iteration and clustering process, and the image features required in the calculation process are highly redundant, which causes the waste of computing resources to some extent. The resolution, contrast and signal-to-noise ratio of microscopic cell images are the main factors affecting segmentation accuracy and efficiency. In this paper, based on microscopic cell images' characteristics, the SLIC algorithm is improved, and the simplified algorithm only needs to calculate the 3-dimensional feature vector, namely the grayscale feature g and spatial feature (x, y), so as to reduce the data dimension. Therefore, the distance between candidate pixel and clustering center of the improved SLIC algorithm is redefined as,

$$d_s(i,j) = \sqrt{(x_i - x_j)^2 + (y_i - y_j)^2} \tag{4}$$

$$d_g(i,j) = \sqrt{(g_i - g_j)^2} \tag{5}$$

$$\dot{d}(i,j) = \sqrt{d_s^2 + \alpha d_g^2} \tag{6}$$

where, i is the label of the clustering center, and j represents the one-dimensional index of all pixels in $2S \times 2S$ neighborhood of the clustering center; $d_s(i,j)$ represents the spatial similarity between pixels; $d_g(i,j)$ represents the gray space similarity between pixels; $\dot{d}(i,j)$ represents the total similarity between the clustering center and pixel points, the smaller the $d'(i,j)$, the more similar the pixel points are to the clustering center. $\alpha = s/m$, s is the size of the neighborhood of clustering center, and m is the compact factor, which is used to control the proportion of $d_s(i,j)$ and $d_c(i,j)$ in $d'(i,j)$, and in general $s \in [1,40]$.

The detailed process of the improved SLIC superpixel segmentation algorithm for segmenting microscopic cell image is as follows,

(1) Firstly, the non-grayscale microscopic cell image is nonlinearly transformed into grayscale image, and then the whole image with n grayscale is randomly divided into K segments. Assuming that the probability distribution of each grayscale is represented as $p_0, p_1, \cdots, p_{n-1}$ respectively, and that the multiple thresholds for optimal classification of each segment is represented as $s_1, s_2, \cdots, s_k, s_1 < s_2 < \cdots < s_k$, so the entropy based on these segments can be expressed as,

$$\begin{aligned}\phi(s_1, s_2, \cdots, s_k) = &\log\left(\sum_{i=0}^{s_1} p_i\right) + \log\left(\sum_{i=s_1+1}^{s_2} p_i\right) + \cdots + \log\left(\sum_{i=s_k+1}^{n} p_i\right) \\ &- \frac{\sum_{i=0}^{s_1} p_i \log p_i}{\sum_{i=0}^{s_1} p_i} - \frac{\sum_{i=s_1+1}^{s_2} p_i \log p_i}{\sum_{i=s_1+1}^{s_1} p_i} - \cdots - \frac{\sum_{i=s_k+1}^{n} p_i \log p_i}{\sum_{i=s_k+1}^{s_1} p_i}\end{aligned} \tag{7}$$

The multiple thresholds $s_1, s_2, \cdots, s_k$ for optimal classification of each segment satisfies the maximum entropy criterion as following formula,

$$(s_1, s_2, \cdots, s_k) = \arg\left\{\max_{s_1, s_2, \cdots, s_k} \left[\phi(s_1, s_2, \cdots, s_k)\right]\right\} \tag{8}$$

and the solution of multiple thresholds is realized by conditional iteration algorithm.

(2) With the multiple thresholds for optimal classification of each segment from the previous step, the image gray level is divided into *K+1* part. Let the gray level interval be expressed as $[X_i, X_{i+1}], X_i \in \{s_1, s_2, \cdots, s_k\}, i \in \{1, 2, \cdots, k\}$, and then transformed the gray scale interval $[X_i, X_{i+1}]$ to the gray scale interval $[Y_i, Y_{i+1}]$ by the gray scale transformation, to achieve the effect of image contrast enhancement and region equalization. The gray scale transformation and equalization operation were completed by monotone transformation function $f(x)$。$f(x)$ is a convexity function in the interval $[X_i, X_m]$, and is a concave function in the interval $[X_m, X_{i+1}]$, the turning point is (X_m, Y_m), where $Y_m = (Y_i + Y_{i+1})/2$, and X_m was calculated according to the least squares principle as follows [28],

$$X_m = \frac{\int_{X_i}^{X_i} x p(x) dx}{\int_{X_i}^{X_i} p(x) dx} \tag{9}$$

To simplify the computational complexity of image gray scale transformation $f(x)$ is set as a continuous analytic function with the following form,

$$f(x) = ax^r + b, x \geq 1, r \geq 1 \tag{10}$$

where $a = (Y_{i+1} - Y_i)/(X_{i+1}^r - X_i^r), b = Y_i - aX_i^r$.

A series of transformation curves can be obtained by changing the parameter *r*. The larger *r* is, the higher the gray equalization degree of the transformed interval $[X_i, X_{i+1}]$is, as shown in Fig. 2.Within the whole gray scale of the cell image, Properly select $Y_i, i \in \{1, 2, \cdots, n\}$ and parameter *r* to transform the gray scale of each interval $[X_i, X_{i+1}]$, then regional balanced and contrast enhanced images can be obtained, and a high regionally equalization and contrast enhanced image can be obtained.

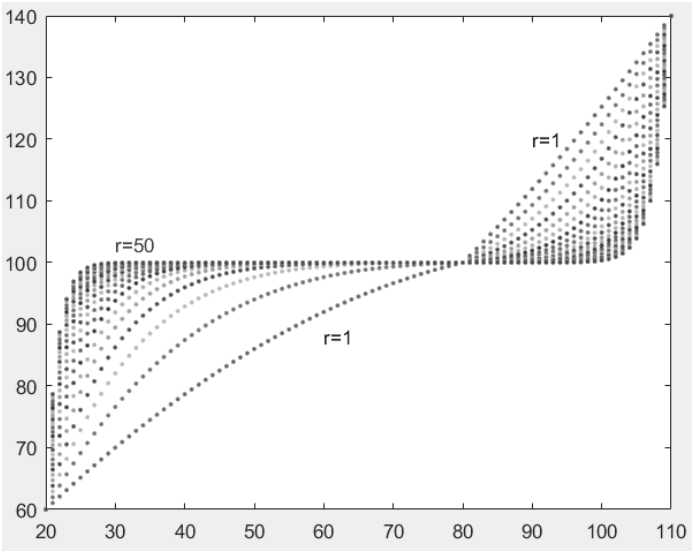

Fig. 2 Examples of grayscale transformation

(3) The clustering center C_i is initialized with the grid superpixel of side length $S = \sqrt{N/M}$, and each clustering center is given a label i;

(4) Move the clustering center C_i to the location with the smallest gradient value in the 3×3 neighborhood centered on it;

(5) Calculate the similarity distance d' from each pixel j to the center C_i in the neighborhood with radius S around each clustering center C_i. Similar pixels can be searched in the circular neighborhood of the clustering center, which can further reduce the calculation amount compared with $2S \times 2S$ neighborhood searching, and the search scope is more in line with the quasi-circular features of the cell image, as shown in figure 1(b).

(6) Let $dist(i)=\infty$, if $d'(i)<dist(i)$ and within the specified range, the $d'(i)$ will be assigned to $dist(i)$, and the label i will be assigned to the neighborhood pixel j;

(7) Repeating the step of (4), (5) and (6) to complete the clustering of the whole image. Then recalculate the mean value of each clustering gray scale and spatial feature after clustering to redefine the clustering center, and repeat iteration until convergence;

(8) Adopting an adjacent merging strategy to merge isolated small size superpixels, to ensure the final result has an excellent close fitting degree.

4. Experimental results and analysis

To verify the validity and performance of the improved SLIC algorithm for segmenting microscopic cell image, we selected two microscopic cell image sets as our experimental data, and these data sets are from ISBI 2019 Cell Tracking Challenge (CTC) competition that provided public data sets (http://celltrackingchallenge.net/) [29,30]. The microscopic cell image sets used in the experiment are all based on image sequence, the two data sets are Fluo-C2DL-MSC and Fluo-N2DL-HeLa, the resolution of each image are respectively 992x832 and 1100x700,and the number of images in the sequence is 48 and 91, respectively.

For microscopic cell image segmentation tasks, the experiment mainly compared the public SLIC segmentation program [24] and the improved SLIC algorithm. In order to quantitatively evaluate the cell segmentation effect of our method, BR (Boundary Recall), ASA (Achievable Segmentation Accuracy) and CUE (Corrected Under segmentation Error) are used to evaluate and analyze the segmentation results of microscopic cell images.BR is a measurement that represents the degree of coincidence between the superpixel segmentation and the manual segmentation boundary, and its calculation formula is as follows,

$$BR(s)=\frac{\sum_{p\in B(g)} I\left[\min_{q\in B(s)}\|p-q\|<\varepsilon\right]}{|B(g)|} \tag{11}$$

where, $B(s)$ and $B(g)$ are the contour sets of manually segmentation and superpixel segmentation, respectively. p is the point on the manual segmentation contour, and q is the point on the superpixel segmentation contour. The function $I[\cdot]$ judges whether a certain point on the superpixel contour is within the distance ε from the point on the current manually segmentation contour [31].

ASA is a kind of measurement on the segmentation accuracy limit, as it was given by using superpixel subunits (that is, instead of pixels) to get the highest precision for image segmentation, its computation formula is as follows,

$$ASA(s)=\frac{\sum_k \max_i |s_k\cap g_i|}{\sum_i |g_i|} \tag{12}$$

It tallies the sum of the manually segmented areas that each superpixel can cover.

CUE can reflect the overlap error between manually segmentation results and superpixel segmentation results. The calculation formula is as follows.

$$CUE(s)=\frac{\sum_k |s_k-g_{\max}(s_k)|}{\sum_i |g_i|} \tag{13}$$

where, s_k represents the superpixel of the kth block, g_i represents the manually divided area of the ith block, and $g_{\max}$ is defined as follows,

$$g_{\max}(s_k)=\arg \max_i |s_k\cap g_i| \tag{14}$$

This expression returns the manually partitioned region between s_k with the maximum intersection.

According to the quantified data in Table 1, when the number of superpixels of Fluo-C2DL-MSC

microscopic cell image to be segmented is set to 1024, 512 and 256, respectively, ISLIC relative to SLIC,BR index increased by 0.83%, 1.47%, 3.73%, ASA index increased by 0.27%, 0.43%, 0.89%, and CUE index decreased by 6.99%, 5.78%, 11.29%, respectively. According to the quantified data in Table 2, when the number of superpixels of Fluo-N2DL-HeLa microscopic cell image to be segmented is set to 880, 440 and 220, respectively, ISLIC relative to SLIC,BR index increased by 2.18%,3.21%,3.84%, ASA index increased by 0.88%,2.69%,3.23%, and CUE index decreased by 10.25%,3.31%,9.51%, respectively. These quantization results show that ISLIC can be effectively applied to the segmentation of microscopic cell images when the appropriate number of superpixels is set according to the image resolution.

Table 1 Segmentation performance measures of original and improved SLIC (ISLIC) applied to Fluo-C2DL-MSC microscopic cell image

Superpixel number	1024		512		256	
Measurement/Method	SLIC	ISLIC	SLIC	ISLIC	SLIC	ISLIC
BR	0.9467	0.9546	0.9168	0.9303	0.8476	0.8792
ASA	0.9536	0.9562	0.9450	0.9491	0.9236	0.9318
CUE	0.0458	0.0426	0.0536	0.0505	0.0797	0.0707

Table 2 Segmentation performance measures of original and improved SLIC (ISLIC) applied to Fluo-N2DL-HeLa microscopic cell image

Superpixel number	880		440		220	
Measurement/Method	SLIC	ISLIC	SLIC	ISLIC	SLIC	ISLIC
BR	0.9571	0.9780	0.9249	0.9546	0.8642	0.8974
ASA	0.9789	0.9875	0.9253	0.9648	0.9395	0.9552
CUE	0.0488	0.0438	0.0514	0.0497	0.0768	0.0695

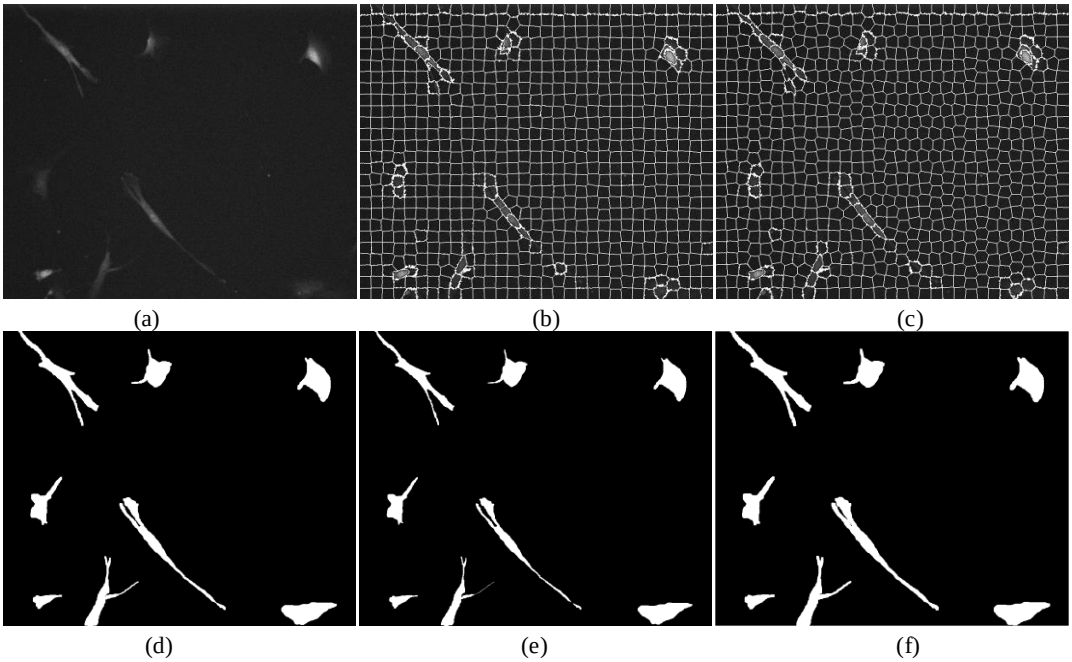

Fig. 3 Segmentation results of different segmentation methods applied to Fluo-C2DL-MSC microscopic cell image. (a) Original cell image; (b) Original SLIC superpixel segmentation; (c) Improved SLIC superpixel segmentation; (d) Manually segmentation result; (e) original SLIC segmentation result; (f) Improved SLIC segmentation results.

Figure 3 and 4 show a visual comparison of the final segmentation results using the original SLIC

algorithm and the improved SLIC algorithm, respectively. It can be seen that the improved SLIC algorithm is more consistent with the manual segmentation result and effectively avoids the over-segmentation phenomenon in the original SLIC segmentation result. Therefore, the improved SLIC algorithm can better adapt to microscopic cell images' characteristics, with better segmentation effect and more accurate results.

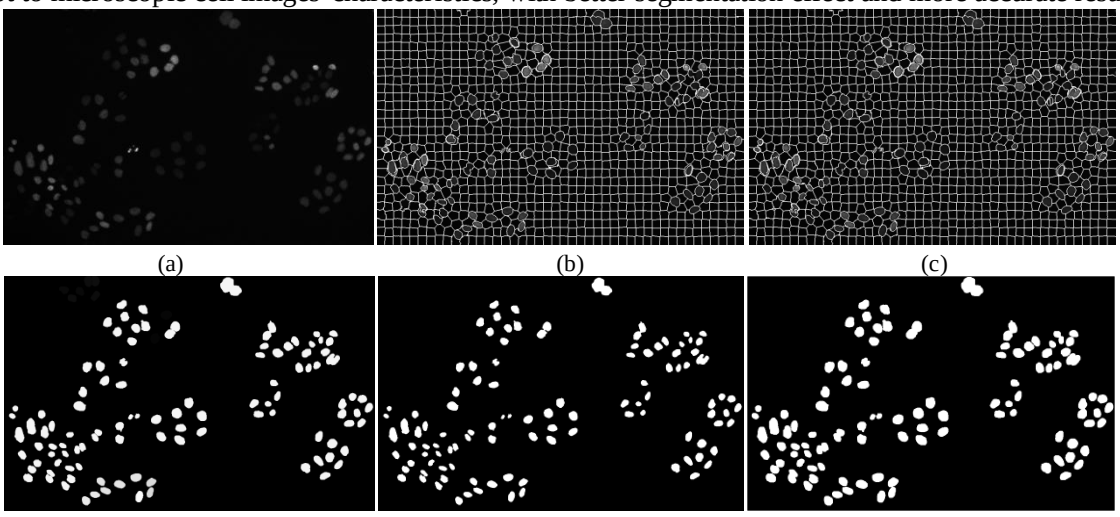

Fig. 4 Segmentation results of different segmentation methods applied to Fluo-N2DL-HeLa microscopic cell image. (a) Original cell image; (b) Original SLIC superpixel segmentation; (c) Improved SLIC superpixel segmentation; (d) Manually segmentation result; (e) original SLIC segmentation result; (f) Improved SLIC segmentation results.

5. Conclusion

Aiming at the original SLIC algorithm's deficiency in microscopic cell image segmentation, we proposed an improved SLIC algorithm. Compared to the original SLIC algorithm with 5D superpixel similarity calculation, our improved SLIC algorithm firstly used conditional iteration algorithm to calculate the multiple optimal image classification threshold based on the maximum entropy principle, then the gray scale transformation was carried out within the classified region, which achieves the effect of image contrast enhancement and region equalization. By the mentioned above preprocessing of microscopic cell image, improved SLIC algorithm calculated superpixel similarity with only the pixel gray and location information, which can effectively reduce the size of the data processing to improve the segmentation accuracy, it also provides an effective method for cell and nucleus segmentation model of microscopic images. Compared with the original SLIC algorithm, the improved SLIC algorithm is simple in a calculation, low in sensitivity to local noise and effectively reduces over-segmentation. In the future, superpixels will be merged and classified on the basis of superpixel segmentation to study the detection, screening and classification of cell targets.

Acknowledgement

This work is supported by the National Natural Science Foundation of China (62062014), the Natural Science Foundation of Guangxi (2018GXNSFAA050024, 2018GXNSFAA294142), Key Laboratory for the Chemistry and Molecular Engineering of Medicinal Resources (Guangxi Normal University), Ministry of Education of China (CMEMR2015B11), Guangxi Key Laboratory of Automatic Detection Technology and Instrument (YQ20202), Guangxi Key Laboratory of Wireless Wideband Communication and Signal Processing (GXKL06180204), and Key Scientific Research Project of Guangxi Normal University (2018ZD007).We gratefully appreciate the invaluable comments from editors and anonymous reviewers.

Reference

[1] Gurcan, Metin N., et al. "Histopathological Image Analysis: A Review." IEEE Reviews in Biomedical Engineering 2(2009):147-171.

[2] Albayrak, Abdulkadir, and G. Bilgin. "Automatic cell segmentation in histopathological images via two-staged superpixel-based algorithms." Medical and Biological Engineering and Computing (2019).

[3] Wang, Pin, et al. "Feature-based analysis of cell nuclei structure for classification of histopathological images." Digital Signal Processing78 (2018):S1051200418300903.

[4] Daud, Nhm, et al. "Segmentation Technique for Nucleus Detection in Blood Images for Chronic Leukaemia." Journal of Physics: Conference Series 1755.1(2021):012053 (9pp).

[5] Somasundaram, D., S. Gnanasaravanan, and N. Madian. "Automatic segmentation of nuclei from pap smear cell images: A step toward cervical cancer screening." International Journal of Imaging Systems and Technology 2(2020).

[6] Ejegwa, P. A. "On Intuitionistic Fuzzy Multisets Theory and Its Application in Diagnostic Medicine." (2017).

[7] Xing, F., and L. Yang. "Robust Nucleus/Cell Detection and Segmentation in Digital Pathology and Microscopy Images: A Comprehensive Review." IEEE Rev Biomed Eng (2016):234-263.

[8] Ronneberger, Olaf. Fischer and T. Brox. "U-Net: Convolution Networks for Biomedical Image Segmentation." International Conference on Medical Image Computing & Computer-assisted Intervention 2015.

[9] He, Fuyun, et al. "Parameter estimation method for blurred cell images from fluorescence microscope." Optical Engineering 55.10(2016):103102.

[10] Makem, M., and A. Tiedeu. "An efficient Algorithm for Detection of White Blood Cell Nuclei Using Adaptive three stage PCA-based fusion." Informatics in Medicine Unlocked (2020):100416.

[11] Gregoretti F, Cesarini E, Lanzuolo C, Oliva G, Antonelli L. An Automatic Segmentation Method Combining an Active Contour Model and a Classification Technique for Detecting Polycomb-group Proteins in High-Throughput Microscopy Images. Methods Mol Biol. 2016; 1480:181-97. Doi: 10.1007/978-1-4939-6380-5_16.

[12] Rajinikanth, V., J. P. Aashiha, and A. Atchaya. "Gray-Level Histogram based Multilevel Threshold Selection with Bat Algorithm." International Journal of Computer Applications93.93 (2014):1-8.

[13] Mitko, Veta, et al. "Automatic Nuclei Segmentation in H&E Stained Breast Cancer Histopathology Images." PLoS ONE8.7 (2013):e70221-.

[14] Prochel, Jan, and B. H. Burda. "Morphology of the carpal region in some rodents with special emphasis on hystricognaths." Acta Zoologica 95.2(2014):220-238.

[15] Christ, P. F., et al. "Automatic Liver and Lesion Segmentation in CT Using Cascaded Fully Convolutional Neural Networks and 3D Conditional Random Fields." International Conference on Medical Image Computing and Computer-Assisted Intervention (2016).

[16] Sun, H. Q., and Y. J. Luo. "Adaptive watershed segmentation of binary particle image." Journal of Microscopy 233.2(2009):5.

[17] Zhou, X., et al. "SSG: superpixel segmentation and Grab Cut-based salient object segmentation." The Visual Computer 11(2018):1-14.

[18] Wang, J., et al. "Visual object tracking with multi-scale superpixels and color-feature guided Kernelized correlation filters." Signal Processing Image Communication 63(2018).

[19] Yang, Xulei, et al. "A Novel Multi-task Deep Learning Model for Skin Lesion Segmentation and Classification." (2017).

[20] Yang, Fan, H. Lu, and M. H. Yang. "Robust Superpixel Tracking." IEEE Transactions on Image

Processing23.4 (2014):1639-1651.
[21] Xu, Jun, et al. "A weighted mean shift, normalized cuts initialized color gradient based geodesic active contour model: applications to histopathology image segmentation." (2010).
[22] Li, Yong, and et al. "An Improved Mean Shift Segmentation Method of High-Resolution Remote Sensing Image Based on LBP and Canny Features." Applied Mechanics and Materials 713-715 (2015):1589-1592.
[23] Çiğla, Cevahir, and A. A. Alatan. "Efficient graph-based image segmentation via speeded-up turbo pixels." IEEE International Conference on Image Processing IEEE, 2010.
[24] Achanta, R., et al. "SLIC Superpixels Compared to State-of-the-Art Superpixel Methods." IEEE Transactions on Pattern Analysis and Machine Intelligence 34.11(2012):2274-2282.
[25] Albayrak, A., and G. Bilgin. "Automatic cell segmentation in histopathological images via two-staged superpixel-based algorithms." Medical & Biological Engineering & Computing 57(2019).
[26] Achanta, R., et al. "SLIC Superpixels Compared to State-of-the-Art Superpixel Methods." IEEE Transactions on Pattern Analysis & Machine Intelligence 34.11(2012):2274-2282.
[27] Quesada-Barriuso, P., D. B. Heras, and F Argüello. "GPU accelerated waterpixel algorithm for superpixel segmentation of hyperspectral images." The Journal of Supercomputing 4704(2021):1-13.
[28] Mahmoudi, L., and A. E. Zaart. "A survey of entropy image thresholding techniques." International Conference on Advances in Computational Tools for Engineering Applications IEEE, 2012.
[29] "A benchmark for comparison of cell tracking algorithms." Bioinformatics 30.11(2014):1609-1617.
[30] "An objective comparison of cell-tracking algorithms." Nature Methods (2017).
[31] Wang, Wei, et al. "Superpixel Segmentation of Polarimetric SAR Images Based on Integrated Distance Measure and Entropy Rate Method." IEEE Journal of Selected Topics in Applied Earth Observations and Remote Sensing (2017):1-14.